Lab on a Chip

PAPER

View Article Online
View Journal | View Issue

Cite this: *Lab Chip*, 2024, **24**, 4288

Skin-interfaced microfluidic biosensors for colorimetric measurements of the concentrations of ketones in sweat†

Yunyun Wu,[ab] Xinming Li,[abc] Kenneth E. Madsen,[abd] Haohui Zhang,[e] Soongwon Cho,[ab] Ruihao Song,[ab] Ravi F. Nuxoll,[abfg] Yirui Xiong,[ab] Jiaqi Liu,[ab] Jingyuan Feng,[abf] Tianyu Yang,[ab] Kaiqing Zhang,[eh] Alexander J. Aranyosi,[abi] Donald E. Wright,[i] Roozbeh Ghaffari,[abci] Yonggang Huang,[aefj] Ralph G. Nuzzo*[d] and John A. Rogers *[abcfk]

Ketones, such as beta-hydroxybutyrate (BHB), are important metabolites that can be used to monitor for conditions such as diabetic ketoacidosis (DKA) and ketosis. Compared to conventional approaches that rely on samples of urine or blood evaluated using laboratory techniques, processes for monitoring of ketones in sweat using on-body sensors offer significant advantages. Here, we report a class of soft, skin-interfaced microfluidic devices that can quantify the concentrations of BHB in sweat based on simple and low-cost colorimetric schemes. These devices combine microfluidic structures and enzymatic colorimetric BHB assays for selective and accurate analysis. Human trials demonstrate the broad applicability of this technology in practical scenarios, and they also establish quantitative correlations between the concentration of BHB in sweat and in blood. The results represent a convenient means for managing DKA and aspects of personal nutrition/wellness.

Received 10th July 2024,
Accepted 14th August 2024

DOI: 10.1039/d4lc00588k

rsc.li/loc

Tribute to George Whitesides

George: I am so grateful that you gave me the opportunity to join your group back in 1995, as a Junior Fellow with financial support through the Harvard University Society of Fellows. (I hope that the prospect for free labor was not a dominating consideration in your decision to let me in!) Your guidance during my two years in your group dramatically influenced the way that I think about academic research, and it set me on a path that I am still following today – beginning with my time at Bell Labs and extending through my academic career at the Univ of Illinois and now at Northwestern. Among the many valuable lessons in scientific writing, academic rigor, intellectual curiosity and interdisciplinary collaboration, perhaps the most important insight that I gleaned from you was a perspective on how to down-select across different possible directions for research – specifically, by prioritizing the pursuit of scientific questions that are not only of fundamental interest but whose answers have the realistic potential to produce outcomes with lasting significance. In many cases, this powerful approach configures efforts around grand challenges for broad segments of society, rather than monodisciplinary topics for narrow academic audiences. For this style of work, you've set an impossibly high standard, but one that we all find profoundly inspiring! Thank you for your support and mentorship over the years and congratulations on your incredible, still-growing scientific legacy – and happy birthday! John Rogers

[a] *Querrey Simpson Institute for Bioelectronics, Northwestern University, Evanston, IL 60208, USA. E-mail: jrogers@northwestern.edu*
[b] *Center for Bio-Integrated Electronics, Northwestern University, Evanston, IL 60208, USA*
[c] *Department of Biomedical Engineering, Northwestern University, Evanston, IL 60208, USA*
[d] *Department of Chemistry, University of Illinois Urbana-Champaign, Urbana, IL 61801, USA. E-mail: r-nuzzo@illinois.edu*
[e] *Department of Civil and Environmental Engineering, Northwestern University, Evanston, IL 60208, USA*
[f] *Department of Materials Science and Engineering, Northwestern University, Evanston, IL 60208, USA*
[g] *Department of Physics and Astronomy, Northwestern University, Evanston, IL 60208, USA*
[h] *State Key Laboratory of Structural Analysis, Optimization and CAE Software for Industrial Equipment, Department of Engineering Mechanics, Dalian University of Technology, Dalian, 116024, Liaoning, China*
[i] *Epicore Biosystems, Inc., Cambridge, MA 02139, USA*
[j] *Department of Mechanical Engineering, Northwestern University, Evanston, IL 60208, USA*
[k] *Department of Neurological Surgery, Northwestern University, Evanston, IL 60208, USA*

† Electronic supplementary information (ESI) available. See DOI: https://doi.org/10.1039/d4lc00588k

Introduction

Ketone bodies including beta-hydroxybutyrate (BHB), acetoacetate and acetone are produced in the liver because of fatty acid oxidation, as an alternative energy source in response to glucose deficiency.[1,2] BHB, as one of the most abundant ketones, is an important biomarker used to clinically diagnose and monitor the status or severity of conditions related to diabetes, complications associated with ketogenic diets, alcoholism, glycogen storage disease and salicylate poisoning.[3] Recent studies indicate that plasma BHB can serve as a biomarker to predict disease progression in patients with arrhythmogenic cardiomyopathy.[4] In healthy people, the concentration of BHB ([BHB]) in blood is low, ranging from 0–0.25 mM.[5] Elevated concentrations can cause an acid–base imbalance which is potentially fatal, as in diabetic ketoacidosis (DKA) with diabetes patients[2,6] or with individuals engaged in ketogenic diets designed to induce ketosis for weight management or obesity treatment.[7,8] Monitoring [BHB] using point-of-care devices can be important in detecting early signs of DKA and in providing insights for dietary interventions.

Conventional methods to monitor DKA and ketosis rely on measurements of ketones in urine and blood.[9–11] The processes for collecting samples of these biofluids are, however, inconvenient and can be performed only episodically. Eccrine sweat, by contrast, can be captured easily and non-invasively, as a rich source of metabolites, electrolytes, hormones, proteins and exogenous agents.[12] Recent advances in soft, skin-interfaced wearable systems enable colorimetric, fluorometric and/or electrochemical *in situ* measurement of a range of sweat biomarkers,[13–16] such as chloride,[17–19] glucose,[20,21] cortisol,[22] nutrients,[23] amino acid,[24] protein,[25] ammonia,[26] creatinine and urea.[27] The results show promising potential for using sweat as a biofluid for disease diagnosis and health management. Existing systems of this type for measuring sweat [BHB] require, however, electrochemical detection schemes with associated electronics for signal acquisition and wireless transmission, and with batteries for power supply.[28,29] Soft, skin-interfaced alternatives that incorporate passive microfluidic constructs and colorimetric chemical assay offer advantages in cost, manufacturability and user factors. In fact, commercial products of this general type are now available for monitoring sweat and electrolyte loss to guide precision replenishment strategies in competitive sports and athletics.[30]

Here we report extensions of this class of platform that enable measurements of sweat [BHB] from microliter volumes collected in microreservoirs that contain paper-based colorimetric enzymatic BHB assays. Detailed studies confirm accurate evaluations in the presence of various interfering species that can appear in sweat. Human trials of the devices on different body locations and with various sweat stimulation methods demonstrate broad applicability in many practical scenarios. Additional studies establish correlations between sweat [BHB] and blood [BHB] in eight human subjects before and after ketone ester (KE) intake and in one subject on a ketogenic diet. The results collectively suggest a cost-effective, easy-to-use method for tracking [BHB] without the need for urine or blood sampling, laboratory facilities or trained personnel.

Results and discussion

Soft, skin-interfaced microfluidic platform integrated with colorimetric BHB assay

As shown in the schematic illustration of Fig. 1a, the soft, skin-interfaced device consists of two major components: the microfluidic structures and the colorimetric BHB assay. The former includes channels, reservoirs and valves designed to capture and route sweat, formed by casting polydimethylsiloxane (PDMS) against 3D-printed molds and then capping the entire structure with a thin, uniform layer of PDMS. The latter resides in the reservoir, to enable determination of the [BHB] in sweat (Fig. S1†). The low modulus, elastomeric properties of the devices facilitate conformal and water-tight contact with the skin, enabled by a thin layer of medical grade double-sided adhesive for efficient capture of sweat as it emerges from the surface of the skin (Fig. 1b–e). Pressure associated with the action of eccrine glands[31] pushes sweat through an inlet port at the skin interface, through microscale channels to the reservoir with colorimetric reagents for detecting BHB. After the reservoir fills with sweat, any excess sweat exits through the outlet due to the use of the capillary bursting valves (CBVs) (Fig. 1f–h).[32,33] This setup avoids continuous flow of sweat through the reservoir, thereby preventing cross-contamination of new sweat with old sweat.

Quantitative colorimetric analysis of BHB

Quantitative measurements of [BHB] in sweat rely on a paper assay (Keto-Test) coated with colorimetric reagents for detecting BHB (Fig. 2a). The porous structure of the paper assays enables fast absorption of sweat due to capillary wicking. The sensing process involves selective enzymatic reaction of the BHB with beta-hydroxybutyrate dehydrogenase enzyme (BHBDH) (Fig. 2b). BHBDH catalyzes the oxidation of BHB to acetoacetate. Concomitantly, the coenzyme nicotinamide adenine dinucleotide (NAD+) converts to its reduced form NADH. The NADH reduces nitrotetrazolium blue to formazan, a compound with a purple color. Analysis of the intensity of this color quantitatively yields [BHB]. Pictures of this assay captured at different times after exposure to a range of concentrations of aqueous BHB solutions are in Fig. 2c. Digital images collected using a digital single-lens reflex (SLR) camera with a color reference chart (ColorChecker) allow for extraction of color information using algorithms based on the CIELAB color space. This scheme defines colors as mathematical combinations of three orthogonal components, L* (lightness), a* (redness), and b* (yellowness). As [BHB] increases, L* decreases, a* increases and b* decreases (Fig. 2d and S2a and b†). In all concentrations, the color responses stabilize in ~10 minutes. Graphing the lightness values at ~10 min as a function of [BHB] between 0 and 0.5 mM reveals a linear correlation with correlation coefficient $R^2 = 0.98$. To eliminate the dependence on lighting conditions, analysis in practical scenarios uses the difference in lightness between the white background of the microfluidic device and the colorimetric assay, with a

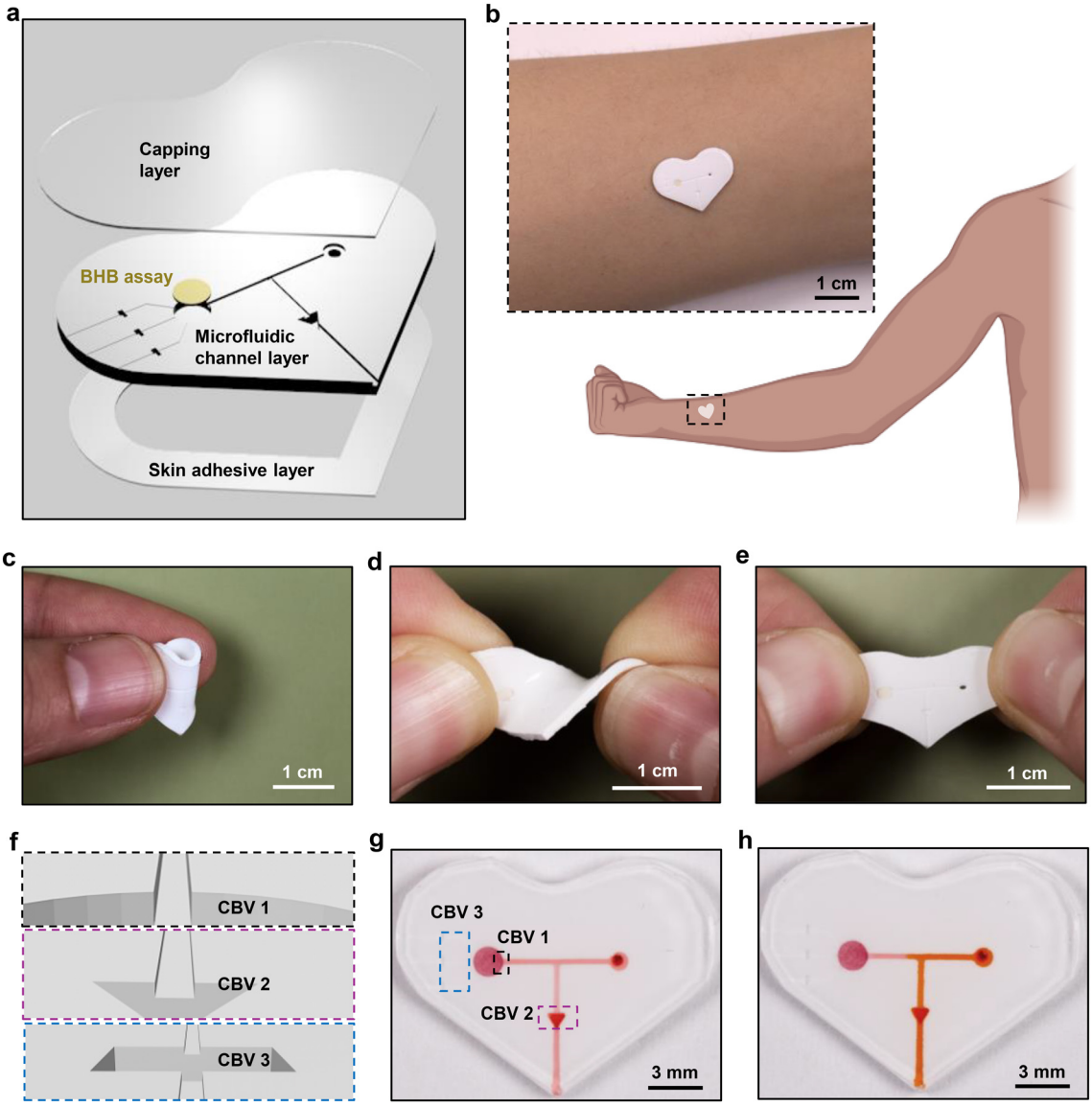

Fig. 1 Schematic illustrations and images of a soft, skin-interfaced microfluidic device for colorimetric analysis of BHB in sweat. a) Exploded view schematic illustration of the capping layer, microfluidic channel structure with BHB assay and the skin adhesive. b) Schematic illustration and image of a device on the forearm. c–e) Images of a device during c) folding, d) twisting and e) stretching. f) Schematic illustration of the CBVs used in a device. g and h) Images of the operation of the CBVs for routing sweat into the microfluidic channel and reservoir. Food dyes were used to enhance visualization. The microfluidic device was initially filled with a solution dyed pink, representing the initial sweat filling. The same device was then further filled with an orange dyed solution to simulate additional sweat collection.

corresponding calibration curve (Fig. S2c†). Based on the standard deviation of the response and the slope of the calibration curve, the calculated limit of detection using the equation of 3.3σ/slope (σ: the standard deviation of y-intercepts of the calibration curve; the slope of the calibration curve) is ~0.01 mM.

The size of the reservoir (reaction zone) plays a key role in the uniformity of color across the area of the assay, an important factor in accurate quantitative analysis.[34] Image analysis shows that the relative standard deviation (RSD) values of color gradients on assays with diameters of 2.5 mm, 2.0 mm, and 1.5 mm are 4.7%, 2.2% and 1.0%, respectively (Fig. 2e). The decrease of RSD corresponds to an increase in uniformity with decreasing diameter, consistent with the results of simulations based on a convection–diffusion model (Fig. 2e). Reaction of most of the BHB occurs near the entrance of the reservoir, thereby producing the purple formazan product in this region. The unreacted BHB diffuses to the remaining part of the assay. Increasing the diameter of the assay increases the time required for filling, thereby leading to increased [BHB] near the entrance and increased color gradients. In experiments, an additional consideration is that the flow of sweat can transport formazan toward the center of the assay, to produce a whitish color near the entrance.

Experiments conducted with samples that include common constituents of human sweat at concentrations within the physiological range, including artificial sweat purchased from Pickering Laboratories (the composition of the artificial sweat

listed in supporting information), solutions of 0.1 mM ascorbic acid, 0.2 mM glucose and 0.02 mM Cu, yield information on the selectivity of the BHB assay (Fig. 2f). The results in all cases indicate negligible interference from these species. Additional measurements indicate consistent results across a range of pH values from 4.4 to 8 (Fig. 2g). Results obtained at temperature from 22 °C to 38 °C reveal only a slight dependence of the response on temperature (Fig. S3†), negligible for most practical purposes.

Sweat generation, collection and colorimetric analysis of [BHB] in human trials

Evaluations in human trials demonstrate the utility of this platform. Sweating can be initiated through active perspiration (physical exercise), thermal stimulation (exposure to a sauna or warm shower) and chemical induction (iontophoretic delivery of pilocarpine), each with utility in different use scenarios. Measurements of sweat [BHB] generated using the three approaches including four methods mentioned from three subjects show insignificant variation within normal ranges (Fig. 3a and b).[28] For example, the average sweat [BHB] of subject 1 are 33 ± 6 μM during exercise, 52 ± 6 μM during sauna, 43 ± 4 μM after a hot shower and 46 ± 8 μM after iontophoresis. Studies with devices placed on four different positions of the body (right forearm, left forearm, chest and back) reveal different sweat [BHB] within the normal ranges (Fig. 3c and d).[28] For example, the average sweat [BHB] of subject 1 during exercise are 33 ± 6 μM from the right forearm, 17 ± 3 μM from the left forearm, 53 ± 5 μM from the chest and 51 ± 6 μM from the back. Analysis of sweat samples collected from subjects using nuclear magnetic resonance (NMR)

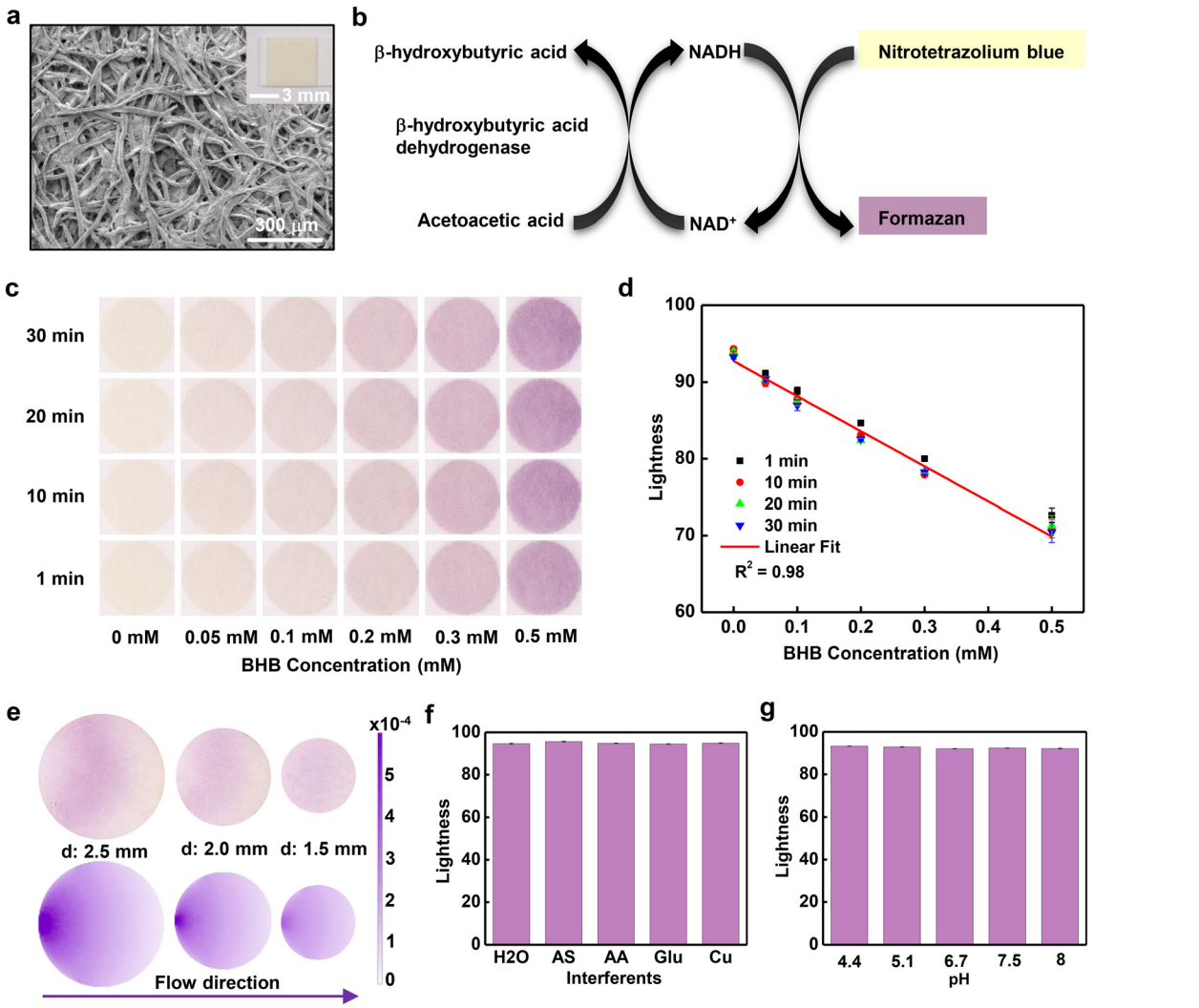

Fig. 2 Quantitative colorimetric analysis of [BHB] by optical image processing. a) Scanning electron micrograph of the BHB colorimetric paper assay. Inset: Image of a BHB test strip. b) Schematic illustration of the operating principles of the BHB assay. c) Images of the BHB assay captured at different times after introduction of solutions of BHB with various concentrations. The diameter of the circular assays is 1.5 mm. d) Lightness L* values extracted from images of BHB assays as a function of time for various concentrations of BHB. e) Experimental results of the distribution of color across BHB assays with diameters of 2.5 mm, 2.0 mm and 1.5 mm along with the corresponding numerical results of the distribution of the total reacted amount of BHB. The color scale bar represents the total reacted amount of BHB. f and g) Lightness L* values for various tested f) interferents and g) pH.

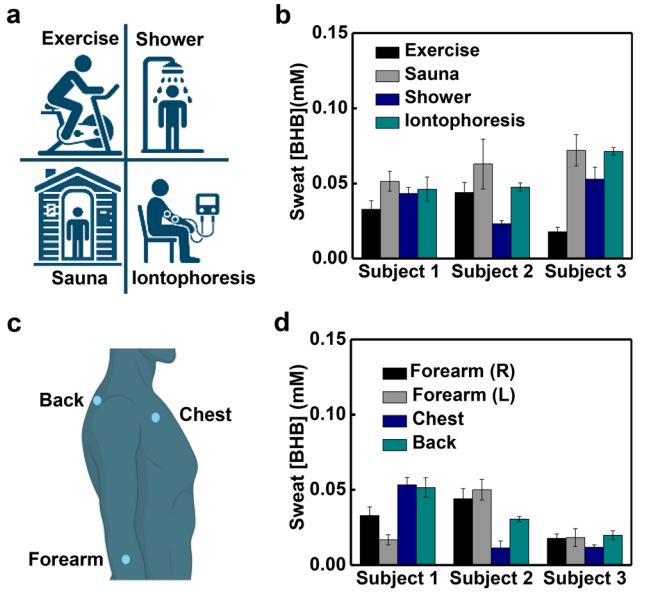

Fig. 3 Sweat generation, collection and colorimetric analysis of [BHB] in human trials. a) Schematic illustration of four different sweat generation methods. b) Measured [BHB] in sweat generated from three subjects using various sweat generation methods. c) Schematic illustration of various locations for mounting the devices. d) Measured [BHB] in sweat generated from various body locations of three subjects during exercise.

spectroscopy and the skin-interfaced microfluidic devices shows comparable results (Fig. S4†).

Study of correlations between sweat [BHB] and blood [BHB] in human trials

Studies of correlations between sweat [BHB] and blood [BHB] use a KE supplement drink to induce changes in the blood [BHB] in a controlled manner. Analysis of blood [BHB] uses a commercial ketone meter (Keto-Mojo) with blood collected from the fingertip of each subject using a sterile lancet. Analysis of sweat [BHB] uses devices applied to the right forearms of subjects after iontophoretic delivery of pilocarpine. Fig. 4a–h shows the results. Before KE intake, the [BHB] are 0.1–0.2 mM in blood and 0.05–0.1 mM in sweat. After ~7.5 g of KE intake, the blood [BHB] increases to 1–2.4 mM and sweat [BHB] increases to 0.23–0.31 mM concomitantly for subject 1–7 (Fig. 4a–g). *Via* consuming various amounts of KE drink (2.5 g, 5 g, 7.5 g and 10 g), the blood [BHB] increases to different levels (0.3 mM, 1.2 mM, 1.8 mM and 3.2 mM). Sweat [BHB] increases accordingly as well (0.096 mM, 0.16 mM, 0.25 mM, and 0.39 mM) (Fig. 4h). Plotting the sweat [BHB] as a function of blood [BHB] reveals a linear correlation with correlation coefficient R^2 = 0.99 (Fig. S5†). [BHB] of sweat induced by exercise, sauna, and shower from the right forearm increases, along with an increase of [BHB] of blood (Fig. S6†). The variations of sweat [BHB] resulted from the body location or sweat induction method before KE intake (Fig. 3b and d) are negligible compared to the changes associated with KE intake. Fig. 4i shows the blood [BHB] and sweat [BHB] from a subject on a ketogenetic diet after iontophoresis. It is observed that the increase of blood [BHB] is along with the increase of the sweat [BHB]. These results suggest correlations between sweat [BHB] and blood [BHB], which is consistent with the previous report.[29]

Conclusions

In summary, this study reports the development and validation of soft, skin-interfaced microfluidic devices that support colorimetric measurement of sweat [BHB]. The design combines an enzymatic BHB paper assay with microfluidic structures to ensure efficient and well-controlled capture of sweat and BHB analysis. Detailed benchtop studies establish capabilities in selective and stable operation across a range of conditions [BHB]. Human trials demonstrate the practical utility of the technology as well as correlations between sweat [BHB] and blood [BHB]. This type of device offers strong potential for broad use in monitoring of DKA and ketosis status.

Experimental

All chemicals were purchased commercially and used as received.

Fabrication of the soft, skin-interfaced microfluidic devices

Fabrication of the devices relied on soft lithography and 3D printing techniques. A 3D printer (Form3B+, Formlabs) formed molds with the geometries of channels and reservoirs. A 5 wt% white silicone dye (Silc Pig White, Smooth-On) mixed with a precursor of PDMS at a 10 : 1 ratio of base to curing agent (Sylgard 184, Dow Corning) served as a white base material. Casting the mixture against the 3D printed molds, removing excess mixture using a razor blade and curing the mixture at ~70 °C for ~1 h yielded stretchable white microfluidic channel layers. A mechanical punch defined 0.5 mm diameter inlet holes. The BHB circular paper assays (diameter of 1.5 mm) cut from BHB test strips (Keto-Test, Elanco) without the sticker material were positioned in the reservoirs. Spin-coating a precursor of PDMS at a 10 : 1 ratio of base to curing agent onto an acrylic wafer at 200 rpm for 30 seconds followed by curing at ~70 °C for ~1 h generated uniform layers of PDMS with thicknesses of ~300 μm as capping layers. Exposing the capping and microfluidic layers to a corona discharge for ~15 seconds (MultiDyne Corona Treating System, 3DT) allowed strong bonds to form between the two upon contact. Application of a medical grade adhesive to the base of the device completed the fabrication.

Characterization of the soft, skin-interfaced microfluidic devices

Calibration experiments and studies of the effect of temperature on the color response of the BHB assay used aqueous solutions of BHB (Sigma-Aldrich) with concentrations between 0 and 0.5 mM, using devices positioned on the surface of a hot plate with temperature monitored using a digital thermocouple (HH374 model, Omega Inc). Solutions with different pH values followed

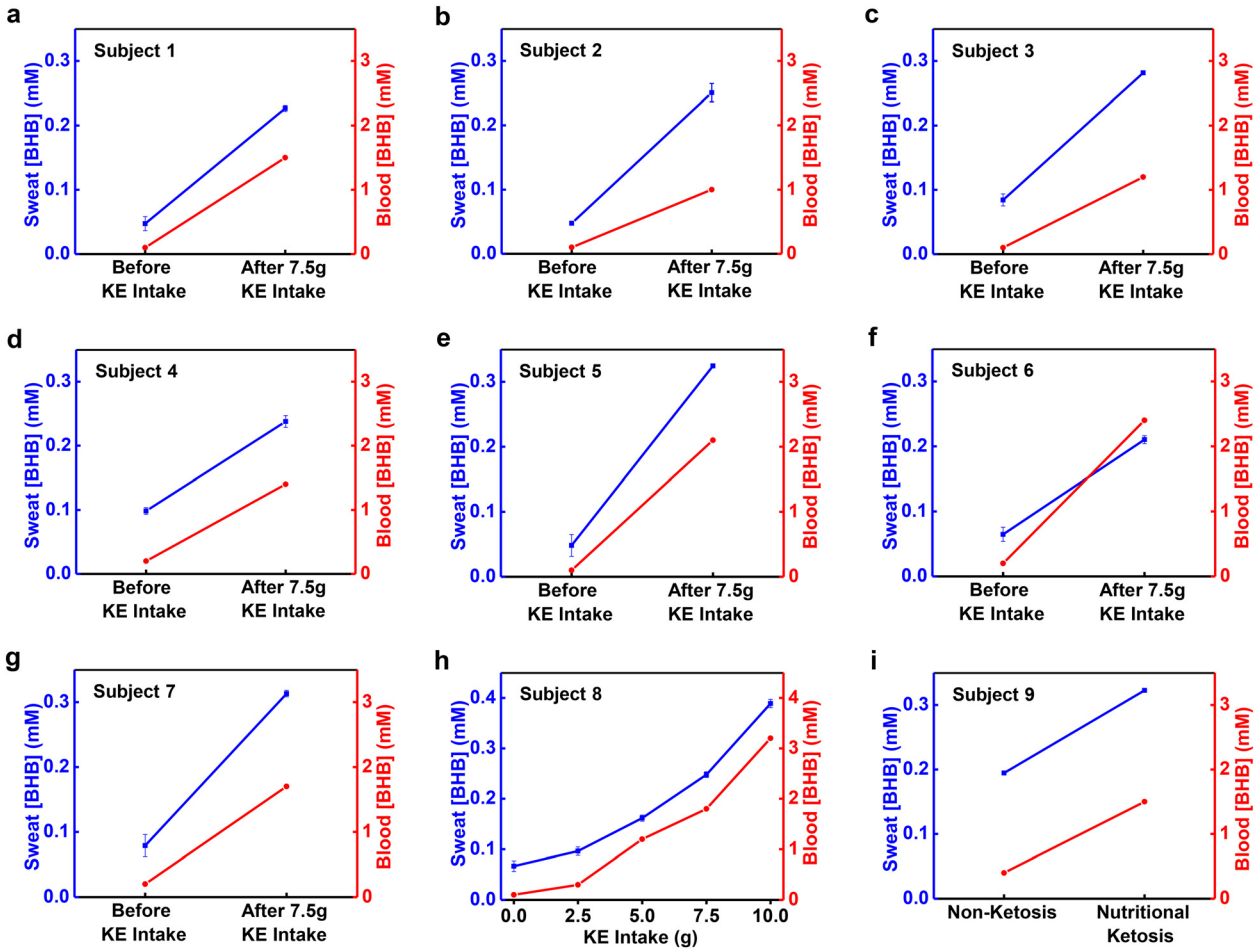

Fig. 4 Study of the correlation between sweat [BHB] and blood [BHB]. a–g) Measured sweat [BHB] and blood [BHB] before and after KE intake from 7 subjects after iontophoresis. h) Measured sweat [BHB] and blood [BHB] before and after taking various amounts of KE drink from subject 8 after iontophoresis. i) Measured sweat [BHB] and blood [BHB] from a subject on a ketogenic diet after iontophoresis.

from the addition of NaOH to BHB solutions in artificial sweat (pH = ~4.5; Pickering Laboratories). Images of the microstructure of the paper BHB assays were captured using a scanning electron microscope (JEOL JSM-7900FLV).

Experimental and numerical studies on the color uniformity of BHB assay

In experiment, a 0.3 mM BHB solution was injected into the microfluidic devices with various diameters (2.5 mm, 2.0 mm and 1.5 mm) using a syringe at a flow rate of 1×10^{-6} L min^{-1} *via* a syringe pump (model Fusion 200, Chemyx Inc). The density and viscosity of water are 1000 kg m^{-3} and 0.001 Pa s, respectively.[35] At a flow rate of 1×10^{-6} L min^{-1} in the experiment, the maximum Reynolds number in the device is 0.11, which is much less than unity such that inertia forces can be neglected. Therefore, the creeping flow model in COMSOL 6.0 can be used to determine the steady-state velocity profile, denoted as $v(x,y)$. The concentration c of BHB within a disk (height 0.15 mm and diameter 1.5 mm/2.0 mm/2.5 mm) is governed by the convection–diffusion equation:

$$-D\nabla^2 c + v\cdot\nabla c = 0$$

where $D = 1 \times 10^{-9}$ m^2 s^{-1} is the diffusivity in water, and v is the steady-state velocity profile solved earlier. The boundary condition at the disk's inlet is that the concentration is c_0 = 0.3 mM, representing the concentration in the sweat. The bottom boundary has a rapid reaction resulting in zero concentration, while all other boundaries have zero diffusive flux.

Images capture and color analysis

The images of microfluidic devices along with a commercial color reference chart (ColorChecker Classic Nano, Calibrite) were captured using digital SLR cameras (EOS 6D or Rebel T6i, Canon). The ColorChecker served as a color reference for color correction/calibration. A python-based ColorChecker program allowed quantitatively analysis of the images. The ColorChecker program maps CIELAB colors in the image color space to colors in a reference color space. The colors of the ColorChecker measured spectrophotometrically by X-Rite define the reference color space. The mapping used an affine

transform. The ColorChecker program yielded the corrected L* (lightness), a* (redness), and b* (yellowness) values of the color from regions of interest. The presented results are the average and standard deviation of 3 separated areas of the captured images.

Sweat stimulation, collection and analysis in human trials

The experimental approach of human trials was reviewed and approved by the Institutional Review Board at Northwestern University with a protocol number of STU00214004-MOD0023. The chemical sweat stimulation occurred on the forearm using the Macroduct Advanced sweat collection system according to the instructions from the manufacturer. Thermal sweat stimulation used a dry sauna setup and a bathroom after a hot shower. Active perspiration followed from cycling exercises. The blood ketone was measured using a commercial ketone meter (Keto-Mojo). Subject consumed 1–4 caps (2.5–10 g) of the ketone ester beverage (KetoneAid KE4) as needed. Sweat collected using the Discovery Patch (Epicore Biosystems) and stored in centrifuge tubes at −20 °C, was quantitatively analyzed for [BHB] using an NMR instrument (NMR HFCN600, Bruker Neo 600 MHz system with QCI-F cryoprobe) and the microfluidic colorimetric devices.

Data availability

Data for this article are available in the main text or the supplementary materials.

Author contributions

Conceptualization: Y. W., J. A. R.; methodology: Y. W., K. E. M., H. Z., S. C., R. S., K. Z., Y. H., R. G. N., J. A. R.; investigation: Y. W., X. L., K. E. M., S. C., R. S., R. F. N., Y. X., J. L., J. F., T. Y.; resources: D. E. W., R. G.; software: A. J. A.; formal analysis: Y. W., X. L.; visualization: Y. W., X. L.; writing – original draft: Y. W.; writing – review & editing: Y. W., X. L., K. E. M., H. Z., A. J. A., R. G., Y. H., J. A. R.; supervision: Y. H., R. G. N., J. A. R.

Conflicts of interest

J. A. R., R. G. and A. J. A. are co-founders of a company (Epicore Biosystems) that commercializes microfluidic devices for sweat analysis.

Acknowledgements

This work was supported by the Center for Bio-Integrated Electronics of Querrey Simpson Institute for Bioelectronics at Northwestern University. This work made use of the EPIC and IMSERC facility of Northwestern University's NUANCE Center, which has received support from the SHyNE Resource (NSF ECCS-2025633), the IIN, and Northwestern's MRSEC program (NSF DMR-1720139).

References

1 M. Evans, K. E. Cogan and B. Egan, *J. Physiol.*, 2017, **595**, 2857–2871.
2 L. Laffel, *Diabetes/Metab. Res. Rev.*, 1999, **15**, 412–426.
3 M. M. Cartwright, W. Hajja, S. Al-Khatib, M. Hazeghazam, D. Sreedhar, R. N. Li, E. Wong-McKinstry and R. W. Carlson, *Crit. Care Clin.*, 2012, **28**, 601–631.
4 J.-P. Song, L. Chen, X. Chen, J. Ren, N.-N. Zhang, T. Tirasawasdichai, Z.-L. Hu, W. Hua, Y.-R. Hu, H.-R. Tang, H.-S. V. Chen and S.-S. Hu, *Sci. Transl. Med.*, 2020, **12**, eaay8329.
5 A. Choi, M. Hallett and D. Ehrlich, *Neurotherapeutics*, 2021, **18**, 1637–1649.
6 K. T. Nguyen, N. Y. Xu, J. Y. Zhang, T. Shang, A. Basu, R. M. Bergenstal, K. Castorino, K. Y. Chen, D. Kerr, S. K. Koliwad, L. M. Laffel, N. Mathioudakis, L. K. Midyett, J. D. Miller, J. H. Nichols, F. J. Pasquel, P. Prahalad, M. R. Prausnitz, J. J. Seley, J. L. Sherr, E. K. Spanakis, G. E. Umpierrez, A. Wallia and D. C. Klonoff, *J. Diabetes Sci. Technol.*, 2022, **16**, 689–715.
7 T. Kelly, D. Unwin and F. Finucane, *Int. J. Environ. Res. Public Health*, 2020, **17**, 2557.
8 F. M. Finucane, M. F. Rafey, M. Leahy, P. O'Shea, T. O'Brien and M. O'Donnell, *Hum. Nutr. Metab.*, 2023, **32**, 200192.
9 R. D. Caño, T. Saha, C. Moonla, E. D. la Paz and J. Wang, *TrAC, Trends Anal. Chem.*, 2023, **159**, 116938.
10 C.-C. Wang, J. W. Hennek, A. Ainla, A. A. Kumar, W.-J. Lan, J. Im, B. S. Smith, M. Zhao and G. M. Whitesides, *Anal. Chem.*, 2016, **88**, 6326–6333.
11 C. Moonla, R. D. Caño, K. Sakdaphetsiri, T. Saha, E. D. la Paz, A. Düsterloh and J. Wang, *Biosens. Bioelectron.*, 2023, **220**, 114891.
12 L. B. Baker, *Temperature*, 2019, **6**, 211–259.
13 A. Koh, D. Kang, Y. Xue, S. Lee, R. M. Pielak, J. Kim, T. Hwang, S. Min, A. Banks, P. Bastien, M. C. Manco, L. Wang, K. R. Ammann, K.-I. Jang, P. Won, S. Han, R. Ghaffari, U. Paik, M. J. Slepian, G. Balooch, Y. Huang and J. A. Rogers, *Sci. Transl. Med.*, 2016, **8**, 366ra165.
14 W. Gao, S. Emaminejad, H. Nyein, S. Challa, K. Chen, A. Peck, H. M. Fahad, H. Ota, H. Shiraki, D. Kiriya, D.-H. Lien, G. A. Brooks, R. W. Davis and A. Javey, *Nature*, 2016, **529**, 509.
15 A. J. Bandodkar, W. J. Jeang, R. Ghaffari and J. A. Rogers, *Annu. Rev. Anal. Chem.*, 2019, **12**, 1–22.
16 J. Min, J. Tu, C. Xu, H. Lukas, S. Shin, Y. Yang, S. A. Solomon, D. Mukasa and W. Gao, *Chem. Rev.*, 2023, **123**, 5049–5138.
17 J. Choi, A. J. Bandodkar, J. T. Reeder, T. R. Ray, A. Turnquist, S. B. Kim, N. Nyberg, A. Hourlier-Fargette, J. B. Model, A. J. Aranyosi, S. Xu, R. Ghaffari and J. A. Rogers, *ACS Sens.*, 2019, **4**, 379–388.
18 T. R. Ray, M. Ivanovic, P. M. Curtis, D. Franklin, K. Guventurk, W. J. Jeang, J. Chafetz, H. Gaertner, G. Young, S. Rebollo, J. B. Model, S. P. Lee, J. Ciraldo, J. T. Reeder, A. Hourlier-Fargette, A. J. Bandodkar, J. Choi, A. J. Aranyosi, R.

Ghaffari, S. A. McColley, S. Haymond and J. A. Rogers, *Sci. Transl. Med.*, 2021, **13**, eabd8109.

19 J. Kim, S. Oh, D. S. Yang, L. Rugg, R. Mathur, S. S. Kwak, S. Yoo, S. Li, E. E. Kanatzidis, G. Lee, H.-J. Yoon, Y. Huang, R. Ghaffari, S. A. McColley and J. A. Rogers, *Biosens. Bioelectron.*, 2024, **253**, 116166.

20 H. Y. Y. Nyein, M. Bariya, L. Kivimäki, S. Uusitalo, T. S. Liaw, E. Jansson, C. H. Ahn, J. A. Hangasky, J. Zhao, Y. Lin, T. Happonen, M. Chao, C. Liedert, Y. Zhao, L.-C. Tai, J. Hiltunen and A. Javey, *Sci. Adv.*, 2019, **5**, eaaw9906.

21 J. Xiao, Y. Liu, L. Su, D. Zhao, L. Zhao and X. Zhang, *Anal. Chem.*, 2019, **91**, 14803–14807.

22 S. Kim, B. Lee, J. T. Reeder, S. H. Seo, S.-U. Lee, A. Hourlier-Fargette, J. Shin, Y. Sekine, H. Jeong, Y. S. Oh, A. J. Aranyosi, S. P. Lee, J. B. Model, G. Lee, M.-H. Seo, S. S. Kwak, S. Jo, G. Park, S. Han, I. Park, H.-I. Jung, R. Ghaffari, J. Koo, P. V. Braun and J. A. Rogers, *Proc. Natl. Acad. Sci. U. S. A.*, 2020, **117**, 27906–27915.

23 J. Kim, Y. Wu, H. Luan, D. S. Yang, D. Cho, S. S. Kwak, S. Liu, H. Ryu, R. Ghaffari and J. A. Rogers, *Adv. Sci.*, 2022, **9**, 2103331.

24 B. Zhong, X. Qin, H. Xu, L. Liu, L. Li, Z. Li, L. Cao, Z. Lou, J. A. Jackman, N.-J. Cho and L. Wang, *Nat. Commun.*, 2024, **15**, 624.

25 J. Tu, J. Min, Y. Song, C. Xu, J. Li, J. Moore, J. Hanson, E. Hu, T. Parimon, T.-Y. Wang, E. Davoodi, T.-F. Chou, P. Chen, J. J. Hsu, H. B. Rossiter and W. Gao, *Nat. Biomed. Eng.*, 2023, **7**, 1293–1306.

26 S. B. Kim, J. Koo, J. Yoon, A. Hourlier-Fargette, B. Lee, S. Chen, S. Jo, J. Choi, Y. S. Oh, G. Lee, S. M. Won, A. J. Aranyosi, S. P. Lee, J. B. Model, P. V. Braun, R. Ghaffari, C. Park and J. A. Rogers, *Lab Chip*, 2019, **20**, 84–92.

27 Y. Zhang, H. Guo, S. B. Kim, Y. Wu, D. Ostojich, S. H. Park, X. Wang, Z. Weng, R. Li, A. J. Bandodkar, Y. Sekine, J. Choi, S. Xu, S. Quaggin, R. Ghaffari and J. A. Rogers, *Lab Chip*, 2019, **19**, 1545–1555.

28 X. Zhang, Y. Xia, Y. Liu, S. M. Mugo and Q. Zhang, *Anal. Chem.*, 2022, **94**, 993–1002.

29 J.-M. Moon, R. D. Caño, C. Moonla, K. Sakdaphetsiri, T. Saha, L. F. Mendes, L. Yin, A.-Y. Chang, S. Seker and J. Wang, *ACS Sens.*, 2022, **7**, 3973–3981.

30 R. Ghaffari, A. J. Aranyosi, S. P. Lee, J. B. Model and L. B. Baker, *Nat. Rev. Bioeng.*, 2023, **1**, 5–7.

31 Z. Sonner, E. Wilder, J. Heikenfeld, G. Kasting, F. Beyette, D. Swaile, F. Sherman, J. Joyce, J. Hagen, N. Kelley-Loughnane and R. Naik, *Biomicrofluidics*, 2015, **9**, 031301.

32 J. Choi, D. Kang, S. Han, S. B. Kim and J. A. Rogers, *Adv. Healthcare Mater.*, 2017, **6**, 1601355.

33 C.-H. Wu, H. J. H. Ma, P. Baessler, R. K. Balanay and T. R. Ray, *Sci. Adv.*, 2023, **9**, eadg4272.

34 W. Tan, L. Zhang, P. Jarujamrus, J. C. G. Doery and W. Shen, *Microchem. J.*, 2022, **180**, 107562.

35 W. M. Haynes, D. R. Lide and T. J. Bruno, *CRC Handbook of Chemistry and Physics: a Ready-Reference Book of Chemical and Physical Data*, CRC Press, Boca Raton, FL, 2016.